

## Sequence Analysis of a “True” Chalcone Synthase (*chs\_H1*) Oligofamily from hop (*Humulus lupulus* L.) and PAP1 Activation of *chs\_H1* in Heterologous Systems

JAROSLAV MATOUŠEK,<sup>†,‡</sup> LUKÁŠ VRBA,<sup>†</sup> JOSEF ŠKOPEK,<sup>†</sup> LIDMILA ORCTOVÁ,<sup>†</sup> KAREL PEŠINA,<sup>†</sup> ARNE HEYERICK,<sup>#</sup> DAVID BAULCOMBE,<sup>§</sup> AND DENIS DE KEUKELEIRE<sup>\*,#</sup>

Biological Centre AS CR, Institute of Plant Molecular Biology, Branišovská 31, 37005 České Budějovice, Czech Republic, Faculty of Biological Sciences, University of South Bohemia, Branišovská 31, 37005 České Budějovice, Czech Republic, Laboratory of Pharmacognosy and Phytochemistry, Faculty of Pharmaceutical Sciences, Ghent University (UGent), Harelbekestraat 72, B-9000 Ghent, Belgium, and The Sainsbury Laboratory, John Innes Centre, Colney Lane, Norwich NR4 7UH, United Kingdom

Screening of a cDNA library of the hop cv. Osvald's 72 and genomic cloning were used to isolate members of an oligofamily of *chs\_H1* genes that codetermine the biosynthesis of prenylated chalcones known to be valuable medicinal compounds present in hop (*Humulus lupulus* L.). *chs\_H1* oligofamily members showed more than 99% and 98% identity on nucleotide and amino acid levels, respectively, and retained all conserved amino acids that form the catalytic center characteristic for “true” chalcone synthases. The *chs\_H1* promoter exhibited low sequence variability in addition to conservation of all predicted cis-regulatory elements. Possible transactivation of the *chs\_H1* gene with the transcription factor PAP1 from *Arabidopsis thaliana* was assayed using *Agrobacterium tumefaciens* infiltrations of *Nicotiana benthamiana* and *Petunia hybrida* plants. Infiltration of *N. benthamiana* leaves with *chs\_H1* promoter/GUS chimeras led to a 24.8-fold increase of the GUS activity when coinfiltrated with the *pap1* gene. Coinfiltration of the “native” *chs\_H1* gene with *pap1* led to an increased accumulation of *chs\_H1* mRNA as observed by semiquantitative reverse transcription–polymerase chain reaction. Transgenic lines of *P. hybrida* expressing the *pap1* gene showed unusual patterns of UV-A-inducible pigmentation and anthocyanin accumulation in parenchymatic and medulla cells. Infiltration of transgenic leaves of *P. hybrida* with *chs\_H1* and *pap1* genes arranged as a tandem led to quick pigmentation within 12 h after UV-A irradiation. It is indicated that the *chs\_H1* promoter contains functional element(s) mediating an efficient response to PAP1 expression and UV-A irradiation. UV-A also induced *chs\_H1* mRNA and accumulation of flavonol glycosides in hop leaves. It can be expected that the PAP1 factor could significantly influence the expression of the *chs\_H1* oligofamily in transgenic hop and modify the hop metabolome.

**KEYWORDS:** Chalcone synthases; transcriptional factors; secondary metabolites; *Humulus lupulus*; hop cDNA library; *Petunia hybrida*; *Nicotiana benthamiana*; plant transformation

### INTRODUCTION

Recent developments in plant biotechnology are based on the knowledge of functional genomics that employ transcriptomics, proteomics, and developing metabolomics to understand the function and regulation of plant genes (for reviews, see 1, 2). The glandular trichomes (lupulin glands) in hop (*Humulus*

*lupulus* L.) form a specific part of the hop metabolome having a relatively stable biochemical composition that can be useful for characterization of hop cultivars and genotypes (3). This stability suggests the possibility of efficiently manipulating the lupulin metabolome by changing structural and regulatory genes using molecular genetic techniques and “Myb” biotechnology approaches using Myb transcription factors as tools for metabolic engineering in plants (4).

Several compounds in the lupulin metabolome are of particular interest in view of their highly interesting medicinal properties (5, 6). In this respect, current research is focused on prenylated flavonoids that constitute a subclass of polyphenols.

\* To whom correspondence should be addressed. Tel: +3292648055. Fax: +3292648192. E-mail: Denis.DeKeukeleire@UGent.be.

<sup>†</sup> Institute of Plant Molecular Biology.

<sup>‡</sup> University of South Bohemia.

<sup>#</sup> Ghent University (UGent).

<sup>§</sup> John Innes Centre.

Xanthohumol (X; up to 1.3%, m/m, of the dry weight of a hop cone) and desmethylxanthohumol (DMX; up to 0.2%) are the principal prenylated chalcones in the lupulin glands. These chalcones are prone to undergoing an intramolecular Michael-type cycloaddition, leading to prenylated flavanones. Thus, X gives rise to isoxanthohumol (IX, the predominant prenylated flavonoid in beer), and DMX leads to a mixture of 8-prenylnaringenin (8-PN) and 6-prenylnaringenin (6-PN). X is a fascinating cancer-chemopreventive compound exhibiting a broad spectrum of inhibition mechanisms at all stages of carcinogenesis (7, 8), while 8-PN is one of the most potent phytoestrogens currently known (9).

The biosynthesis of prenylated chalcones in hop cones is mediated by an enzyme with so-called "true" chalcone synthase (CHS; EC 2.3.1.74) activity, which efficiently catalyzes the production of chalcones by the condensation of three malonyl-CoA units and *p*-coumaroyl-CoA. Further diversification of the biochemical pathway results in the formation of prenylated chalcones including X and DMX by prenylation and methylation reactions. CHS activity has been detected in hop extracts by Zuurbier et al. (10), and the corresponding "true" CHS-encoding gene designated as *chs\_H1* was cloned and characterized in our previous studies (11–14). Moreover, from genomic blots, we detected an oligofamily of *chs\_H1*-related sequences in hops (11, 12). The *chs\_H1* oligofamily has not yet been characterized by sequential analysis, although coexpression of individual members of this oligofamily and their regulation very likely are key factors in understanding the genetically determined levels of prenylated flavonoids in the metabolome of various hop genotypes.

In our previous work, we characterized in detail the 0.5-kb upstream promoter part of the *chs\_H1* gene. On the basis of these sequences, the involvement of cis-regulatory factors (like Mybs) in the regulation of the *chs\_H1* expression was predicted (13). This would imply eventual manipulation of the *chs\_H1* expression by trans-acting heterologous factors that are specific for regulation of the prenylflavonoid pathway in plants. Some factors, including PAP1, ANT, and C1, are known to induce related phenylpropanoid pathway steps in phylogenetically distant species (14–19). For instance, overexpression of the PAP1 factor from *Arabidopsis thaliana* has been shown to activate the production of anthocyanin-derived pigmentation in a heterologous system involving transgenic tobacco (15). Using microarrays and complex analytical approaches, Tohge et al. (20) have recently shown that ectopic PAP1 overexpression in *A. thaliana* led to the induction of 38 genes and the modification of the *A. thaliana* metabolome.

In the present study, we characterized an oligofamily of "true" chalcone synthases in hop and compared four *chs\_H1* cDNA sequences isolated from the cv. Osvald 72, which revealed high sequence identities for individual oligofamily members. Analysis of alternative promoter variants of *chs\_H1* genes also revealed low sequence variabilities and conservation of all cis-binding motifs, suggesting a high functional uniformity within this oligofamily. Using a series of plant expression vectors, we proved the functionality of the isolated *chs\_H1* promoter sequences and the capability of the PAP1 transcription factor from *A. thaliana* to activate the *chs\_H1* gene in the heterologous systems of *Nicotiana benthamiana* and *Petunia hybrida*. This finding suggests that PAP1 biotechnology is apt to modify the hop metabolome via activation of natural *chs\_H1* genes.

## MATERIALS AND METHODS

### Isolation and Cloning of *chs\_H1* Variants and Promoter Sequences.

For isolation of the new *chs\_H1* variants 132 and 211, a hop

cDNA library from lupulin glandular tissue-enriched hop cones of cv. Osvald's clone 72 (13) was screened using a <sup>32</sup>P-labeled *chs\_H1* CDS probe. Clones that were positive after secondary screening were converted from the Uni-ZAP XR  $\lambda$  phage vector to the pBluescript SK(-) (Stratagene, La Jolla, CA) plasmid form, and the insert was sequenced.

A complete *chs\_H1* gene variant 1539 was obtained as a 2.1-kb PCR fragment from Osvald's clone 72 genomic DNA using the primers *chs\_H1-prom-5'* (5'GATCACGACCGTCCATTCTT3') and *chs\_H1-3'* (5'GAAATTGACCTTACTCCAAAAATG3'), and the fragment was cloned blunt end into the *Sma*I site of the pUC19 vector. The promoter of the sequence variant 132, which was most abundant in the hop cDNA library, was obtained by inverse PCR using the primers H1-132InvFor (5'CCACTCCGGCCAACGTG3') and H1-132InvRev (5'GTTTAGTTTAGTAATAGGACTCTACAACAACT3') and digested with *Sac*I and circularized Osvald's clone 72 genomic DNA as the template. The resulting 6-kb fragment was cloned blunt end into the *Sma*I site of pUC19, and the proximal 1.4-kbp part including the promoter and possible upstream elements were sequenced.

**Preparation of Plant Expression Vectors.** PAP1 (AtMyb75) CDS was obtained by reverse transcription–polymerase chain reaction (RT-PCR) from *A. thaliana* var. Columbia RNA using primers PAP5' (5'ATGGAGGGTTCGTCCAAA3') and PAP3' (5'CTAATCAAATT-TCACAGT3'), cloned into the *SrfI* site of the pCRScript vector (Stratagene, Garden Grove, CA), and verified by sequencing. A *Nco*I-*Bam*HI PAP1 fragment containing the complete coding region was cloned in the frame between the CaMV 35S promoter and the polyA signal of the vector pRT-100 (21). This PAP1 expression cassette was then excised with *Hind*III and cloned into the *Hind*III site of the binary vector pLV-07 (22). The vector designated as pLV-51 was introduced into the *Agrobacterium tumefaciens* strain LBA 4404 by the freeze-and-thaw method. The corresponding *A. tumefaciens* strain was maintained in a medium containing 100 mg L<sup>-1</sup> kanamycin. This vector was used for the transformation of petunia plants.

For the infiltration studies, we prepared a series of vectors that could be maintained in vigorous *A. tumefaciens* in EHA101. These vectors were based on a newly prepared binary vector pLV-62. The vector backbone was obtained from pGA-482 to allow for selection of bacteria on tetracycline instead of kanamycin. This backbone fragment having 7 kb and containing the RK2 replication origin and *tetA* gene for resistance against tetracycline was prepared by partial *Sal*I digestion of pGA-482 outside T-DNA and ligated to the annealed oligonucleotide 5'TCGAAGATCT3' in order to replace the *Sal*I site with *Bgl*II. Subsequently, the MB1 origin was ligated to this fragment to allow for a high level of replication in *Escherichia coli*. The MB1 origin was prepared by a high-fidelity *Pwo* polymerase amplification from pCRScript using the following primers: ori*Bgl*II (5'GGAGATCTG-GCGCTTCCGCTTC3') and ori*Bam*HI (5'GCGGATCCTGAGCGT-CAGACCCC3'). The amplified fragment (830 bp) was treated with *Bgl*II and *Bam*HI and fused with the *Bgl*II-predigested backbone, yielding an intermediary vector designated as pLV-60. Finally, the T-DNA part was cut out from the vector pLV-07 (22) as a *Bgl*II fragment and cloned into pLV-60. The resulting vector was designated as pLV-62 and contained the following fusion cassette: MB1 replication origin–*Bgl*II restriction site–right T-DNA border–multicloning site–*npt*II gene–left T-DNA border–*Bgl*II restriction site.

To prepare an expression vector containing *chs\_H1* cDNA driven by the 35S promoter, the *chs\_H1* variant 132 (see above) was reamplified by *Pwo* polymerase with the primers *chs\_H1CDS-Nco*I-5' (5'AT-CCCCATGGTTACCGTCGAGGAAG3') and *chs\_H1-3'* (5'GAAATT-TGACCTTACTCCAAAAATG3'), digested with *Nco*I and *Eco*RV, and ligated into *Nco*I- and *Sma*I-cleaved pRT100. The expression cassette was excised from pRT100 with *Hind*III and cloned into the *Hind*III site of pLV-62, resulting in the binary vector pLV-64. The 35S-driven *pap1* gene from the vector pLV-51 was cloned as a *Asci*–*Pac*I fragment into pLV-62, resulting in the vector pLV-65. The "native" *chs\_H1* gene variant 1539 was excised by *Eco*RI and *Hind*III cleavage from pUC19 and ligated into *Eco*RI- and *Hind*III-digested pLV-62, resulting in the binary vector pLV-66. The preparation of an expression cassette containing the "native" *chs\_H1* gene fused to the 35S-driven *pap1* gene involved digestion of the *chs\_H1* gene variant

1539 in pUC19 by *Eco*RI and partially by *Sal*I and isolation as a 2.13-kb fragment. This fragment was ligated into *Eco*RI- and *Sal*I-digested vector pLV-65. The resulting vector was designated as pLV-67. The promoterless *chs\_H1* gene fragment was obtained by PCR using the primers H1ΔPKpnXho (5'GCGGTACCTCGAGGAAAAATGGTTAC-CGTCG3') and M13reverse (5'GGAAACAGCTATGACCATG3'), and the *chs\_H1* gene variant 1539 in pUC19 was used as the template. The PCR product was digested with *Kpn*I and *Hind*III and ligated into *Kpn*I- and *Hind*III-digested pLV-62, resulting in the binary vector pLV-78.

Vectors pLV-64, -65, -66, -67, and -78 were introduced into the *A. tumefaciens* strain EHA 101 by the freeze-and-thaw method. The corresponding *Agrobacterium* strains were grown in media containing 2.5 mg L<sup>-1</sup> tetracycline and 50 mg L<sup>-1</sup> kanamycin.

To prepare the *chs\_H1-gfp-gus* fusion construct, the promoter region of the original clone *chs\_H1* (AC:AJ304877) was reamplified by *Pwo* polymerase using *chs\_H1-prom-5'* (5'GATCACGACCGTC-CATTCTT3') and CHSstart primer (5'AACCATGGTCCCTTAGTT-CCGAT3'). The promoter fragment was fused via *Nco*I and *Bam*H1 with *gfp* and *gus* genes arranged as a tandem in the vector pBFG-0 (23). The resulting vector pBFG-PH1 was maintained in *A. tumefaciens* LBA 4404.

**Leaf Infiltration, Plant Transformation, and Tissue Culture Conditions.** The method described by Voinnet et al. (24) was applied with minor modifications. Briefly, bacteria (*A. tumefaciens*) containing the expression vector were grown in 20 mL of a LB medium containing either kanamycin (50 mg L<sup>-1</sup>) for LBA 4404 or 50 mg L<sup>-1</sup> kanamycin and 2.5 mg L<sup>-1</sup> tetracycline. Cells were activated in 10 mM MES, pH 5.6, and 10 mM MgCl<sub>2</sub> buffer containing 150 μM acetosyringone overnight. Prior to infiltration of *N. benthamiana* and *P. hybrida* leaves, aliquots of the suspensions were mixed in varying combinations with the pCB301-p19 vector containing the suppressor of post-transcriptional silencing p19 (24). If not otherwise stated, leaves were collected for analysis 5 days post-infiltration.

Petunia plants were cultivated in vitro on 1.0% agar containing an MS medium (25) under conditions described by Vrba and Matoušek (22). Plants were transformed according to a standard leaf disk method (26) and maintained on the medium containing 200 mg L<sup>-1</sup> kanamycin and 200 mg L<sup>-1</sup> timentin.

**RNA Extraction and Semiquantitative (SQ) RT-PCR Analysis.** For the SQ RT-PCR, the total RNA was isolated from 100 mg of plant leaf tissue using CONCERT (Plant RNA Purification Reagent, Invitrogen) following RNA purification and DNA cleavage on columns (RNeasy Plant Total RNA kit, Qiagen, Germany). To analyze the expression of *chs\_H1*, aliquots of RNA samples were applied to RT-PCR using the Titan One Tube RT-PCR System (Roche) with diagnostic primers designated as CHS\_H1 A1 (5'ATCACTGCCGT-CACT TTC3') and CHS\_H1 A2 (5'AAATAAGCCCAGGAACATC3') (J2). The reaction mixture according to the manufacturer's manual was used except that the concentration of the primers was increased to 1.5 μM. Reverse transcription was run for 30 min at 48 °C, and after denaturation at 94 °C for 2 min, PCR was started with cycles of 30 s at 94 °C, 30 s at 55 °C, and 60 s at 68 °C. Aliquots of the PCR product (10 μL) were taken at annealing steps next to the sampling cycles and after completion of the PCR. Electrophoresis was performed in 1.5% agarose gels. For SQ RT-PCR, nucleic acids were transferred by a Southern blot to nylon membranes charge modified at 0.45 μm (Sigma) and hybridized to a [α-<sup>32</sup>P]dCTP-labeled CHS probe. The intensities of the bands on the Southern blots were determined by scanning via a TYPHOON PhosphoImager (Amersham Biosciences, Piscataway, NJ) and quantified using ImageQuant software (Molecular Dynamics, Sunnyvale, CA).

**Genomic Blots and Northern Blot Analysis.** Genomic DNA from petunia leaves was isolated as described by Tai and Tanksley (27). Southern analyses were performed by using Qiabrade Nylon Plus membranes (Qiagen). Hybridization was conducted according to Church and Gilbert (28) at 65 °C in a 0.4 M phosphate buffer, pH 7.2, containing 7% sodium dodecyl sulfate (SDS), 1% bovine serum albumin, 1 mM ethylenediaminetetraacetic acid (EDTA) at pH 8.3, and a [α-<sup>32</sup>P]dCTP-labeled PAP1 cDNA probe. After hybridization over-

night, washing was performed at 65 °C (three times) for 30 min using a 100 mM phosphate buffer at pH 7.2, 1% SDS, and 1 mM EDTA at pH 8.3.

For Northern blot analysis of the PAP1 expression, total RNA samples from petunia tissues were extracted using the CONCERT reagent and dissolved in diethyl pyrocarbonate (DEPC)-treated water. Aliquots of 35 μg were separated on formaldehyde-denaturing agarose gel. After blotting onto Biodyne A transfer membranes (Pall, Hampshire, England), samples were hybridized to a full-length PAP1 cDNA probe labeled with [α-<sup>32</sup>P]dCTP. Prehybridization and hybridization were carried out in a 50% formamide-based (pre)hybridization buffer (29) at 50 °C. The final washing was performed in 0.5×SSC plus 0.1 M SDS at 55 °C for 20 min. PAP1 cDNA probes for Southern and Northern blot analyses were labeled with [α-<sup>32</sup>P]dCTP using the Redivue [α-<sup>32</sup>P] dCTP 3000 Ci mmol<sup>-1</sup> Rediprime II random prime labeling system (Amersham Pharmacia Biotech, Freiburg, Germany). The autoradiograms were scanned using the TYPHOON PhosphoImager.

**Plant Cultivation Conditions, UV-A Irradiation, Sampling, and Analysis of Secondary Metabolites.** *N. benthamiana*, *P. hybrida* cv. Andrea, and Czech semiearly red-bine hop (*Humulus lupulus L.*) Osvald's clone 72 plants (from the Hop Research Institute, Žatec, Czech Republic) were maintained in glass boxes at a temperature of 25 ± 3 °C. Plants were grown under natural light from March to July 2005 with supplementary illumination [170 μmol m<sup>-2</sup> s<sup>-1</sup> PAR] to keep a 16 h day<sup>-1</sup> period. UV-A irradiation of petunia and hop plants was performed using a Black-Ray B100AP long-wave ultraviolet UV lamp (supplied by East Port, Prague, Czech Republic), which provided a concentrated and high-intensity (7000 μW cm<sup>-2</sup>) beam of 365 nm at a distance of 38 cm. If not otherwise stated, plant leaves were exposed to UV-A for 15 min from a distance between 35 and 40 cm.

Leaves of *N. benthamiana*, petunia, and hop were used for protein and RNA extractions immediately after collection. hop leaves were lyophilized prior to analysis of secondary metabolites. Samples of 25–50 mg were extracted in triplicate using 1 mL of a methanol/water mixture (1/1, v/v). After centrifugation and filtration, the sample was analyzed by high-performance liquid chromatography (HPLC) using a Waters 2695 Alliance Separations Module and a Water 996 photodiode array. The column was a Varian Omnispher (C18, 250 × 4.6 mm, 5 μm) and was maintained at 35 °C, while the injection volume was 50 μL. Gradient elution over 60 min was applied from 15% of solvent B (a methanol/acetonitrile mixture with 0.025% formic acid) in solvent A (water with 0.025% formic acid) to 95% of solvent B in solvent A. Chromatograms at 310 and 350 nm were extracted from the 3D data, and peaks were characterized based on their UV spectra and retention times and compared with authentic standards. Peak integrations were carried out using standard parameters, and normalized peak areas were calculated by dividing the peak areas by the sample mass.

**Other Methods.** The GUS activity was measured according to Jefferson (30) on a DyNA Quant 200 fluorimeter (Hoefer), using 1 mM 4-methylumbelliferyl-β-D-glucuronide (MUG) as the substrate. The activity unit was defined as 1 pmol of 4-methylumbelliferyl (MU) per min at 37 °C. The GUS activity was calculated per milligram of fresh mass of leaf tissue.

For the study of anthocyanin localization in petunia tissues, leaf, petiole, and stem, transverse sections (80–100 μm) were prepared using a microtome (Meopta, Přerov, Czech Republic) and analyzed as fresh samples using a light microscope.

For analysis of the pigment production, individual samples were photographed and analyzed with the "measure pixel density" option using *Lucia* version 5.0 software (Laboratory Imaging, Prague, Czech Republic).

Phylogenetic comparisons of chalcone synthases were performed on sequences with the following accession numbers in the EMBL nucleotide database: true chalcone synthase from *Medicago sativa*, AB061021; valerenophenone synthase from *Humulus lupulus*, AB047593; *chs\_H1* from *H. lupulus* AJ304877. Newly described *chs\_H1* variants in this study have the following accession numbers: clone No. 132, AM263200; clone No. 211, AM263201; clone No. 1539, AM263199.

Sequence analyses were carried out with DNASIS for Windows, version 2.6 (Hitachi). The phylogenetic tree was calculated by the

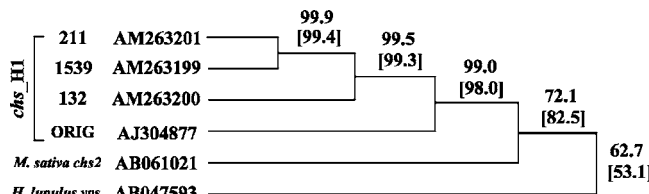


**Figure 1.** Homology tree for cDNA and amino acid sequences of the *chs\_H1* oligofamily members; comparison with "true" chalcone synthase from alfalfa. The tree is rooted using the *chs*-like sequence of valerophenone synthase from hop. Homology percentages are given for nucleotide sequences and, in brackets, for deduced amino acid sequences. The calculations were performed by means of DNAsis for Windows version 2.6 (Hitachi) using the multiple-sequence alignment function. Trees were generated with the Clustal W option of the program.

Neighbor-Joining method in the ClustalW option of the DNAsis software. Amino acid classes described by Bork et al. (31) were used for protein comparisons.

## RESULTS

**Sequence Analysis of the *chs\_H1* Oligofamily.** In our previous work, we have cloned and characterized a "true" chalcone synthase gene designated as *chs\_H1*, and from genomic blots, we predicted the existence of an oligofamily of *chs\_H1*-related genes (11, 12). Consequently, we particularly focused on the sequence analysis and comparisons of *chs\_H1* oligofamily members from the Czech hop cv. Osvald's 72. To obtain additional *chs\_H1* homologues, we initially screened a cDNA library from lupulin glandular tissue-enriched hop cones, which we had established previously (13), with a *chs\_H1*-specific hybridization probe. Sequencing of positive clones revealed two new variants No. 132 and No. 211 having accession numbers AM263200 and AM263201, respectively, which were clearly homologous to the original *chs\_H1* sequence (AJ304877). The sequence of clone 132 appeared to be most abundant in the cDNA library, matching four out of seven fully sequenced positive clones. In parallel experiments, an additional variant No. 1539 was obtained by high-fidelity PCR from Osvald's 72 genomic DNA (AM263199). In total, four sequence variants of the *chs\_H1* coding region were aligned and compared to "true" chalcone synthase from alfalfa, as well as to a CHS-like enzyme, valerophenone synthase from hop (Figure 1). It can be seen that isolated *chs\_H1* oligofamily members show more than 99% and 98% identity on nucleotide and amino acid levels, respectively, within the oligofamily and share more than 82.5% amino acid identity with chalcone synthase from alfalfa, while valerophenone synthase exhibits low homology to the *chs\_H1* oligofamily. Most importantly, all nonhomologous (positions 61, 123, 229, and 236), as well as homologous (positions 211, 302, 308, and 358), amino acid changes occurred out of the set of conserved residues. These residues are characteristic for the "true" chalcone synthase, more specifically for formation of the geometry of the active site, the active center, the cyclization pocket, and the coumaroyl binding site (Figure 2A). These sequence characteristics suggest catalytic conservation of the oligofamily of *chs\_H1* genes.

The sequence of the most abundant variant No. 132 was used to design primers for inverse PCR to obtain and partially sequence a 6-kb fragment upstream of the coding sequence of clone No. 132. Together with the original *chs\_H1* clone (AJ304877), three variants of the *chs\_H1* promoter region were compared. The variability of the promoter sequence is displayed in Figure 2B. The 0.5-kb upstream parts of the No. 132-derived inverse PCR clone and of clone No. 1539 share 99.2% and

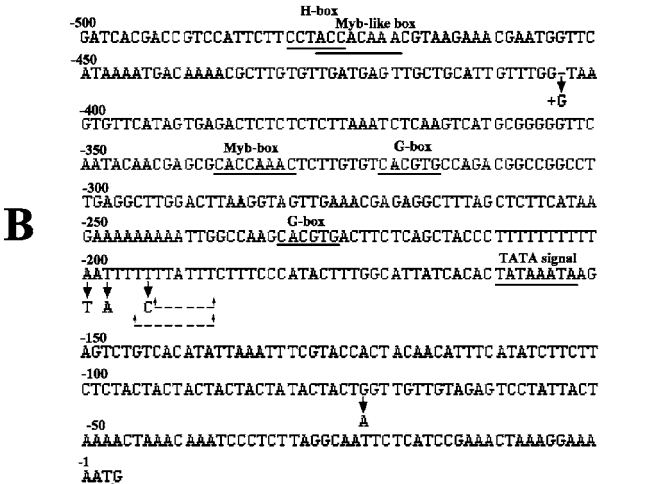
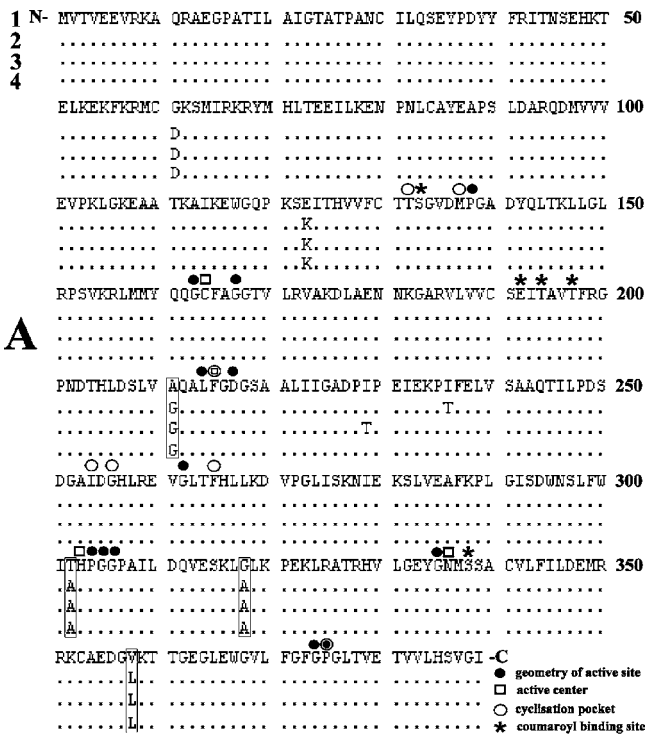


**Figure 2.** Amino acid alignment and sequential analysis of isolated members of the *chs\_H1* oligofamily (A) and nucleotide sequence variabilities within the promoter region of the *chs\_H1* genes (B): 1, the *chs\_H1* amino acid sequence published under AJ304877 in the EMBL database (clone ORIG); 2, clone No. 1539; 3, clone No. 132; 4, clone No. 211. The promoter sequence of clone No. 1539 is shown. Putative regulatory signals, H-boxes, G-boxes, and Myb boxes are according to Rushton and Somssich (32) and Matoušek et al. (13).

98.0% identity, respectively, with the original *chs\_H1*. Except for one base change and one base insertion, most of the variabilities including short deletions occurred in the AT-rich region, which can be identified from nucleotide position -185 to position -211. Isolated sequences of the *chs\_H1* promoter showed a high degree of conservation including all predicted cis-regulatory elements, G-boxes, H-boxes, and Myb binding sites known in the original clone. These results suggest that, in addition to catalytic conservation, the *chs\_H1* oligofamily exhibits a high degree of promoter uniformity.

**PAP1 Activation of Anthocyanin Biosynthesis and Functional Analysis of *chs\_H1* in Heterologous Systems.** According to our previous studies on *chs\_H1* expression and promoter

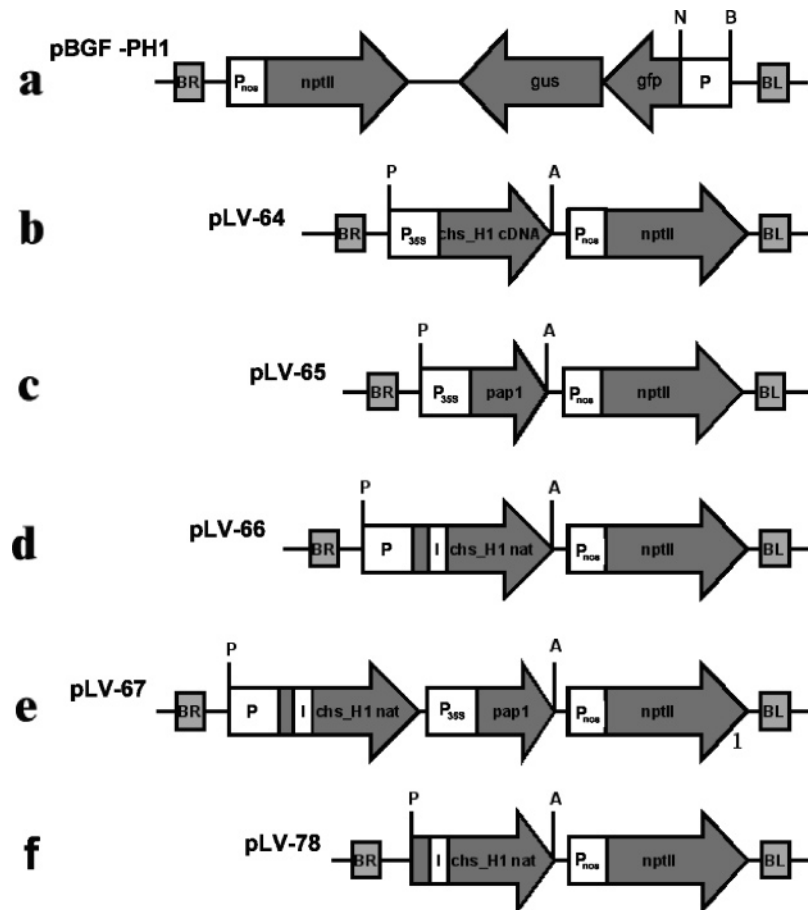


**Figure 3.** Schematic drawing of expression cassettes within the T-DNA parts of the plant vectors used for leaf infiltration. The schemes are not to scale. (a) Vector pBGF-PH1 containing the *chs\_H1* promoter inserted into the pBGF-0 vector via *Nco*I and *Bam*H1 restriction sites. (b–d) Cassettes bearing 35S-driven *chs\_H1*, 35S-driven *pap1*, and the “native” *chs\_H1* gene, respectively. (e) Native *chs\_H1* gene head-to-tail arranged to the 35S-driven *pap1* gene as a tandem. (f) Promoterless “native” *chs\_H1* gene. Coding sequences are in dark gray, promoters and introns are in white, and T-DNA border sequences and multiple cloning sites are in light gray. NptII designates the neomycin phosphotransferase gene for resistance to kanamycin. This gene is driven by the nopaline synthase promoter: I, chalcone synthase intron sequence; BR and BL, right and left T-DNA borders, respectively. By the letters N, B, A, P, the positions of *Nco*I, *Bam*H1, *Ascl*, and *Pad* restriction sites are shown, respectively. These restriction sites were used for the integration genes and cassettes in the plant vector.

composition, we predicted an involvement of *myb*, *myc*, and *b/hh* cis-acting factors in *chs\_H1* regulation (11, 13). Indeed, as demonstrated in this study, the predicted cis-regulatory elements remained conserved within the compared promoter sequences of the *chs\_H1* oligofamily. For instance, a plant-specific *myb* recognition element having consensus A(A/C)C-(A/T)A(A/C)C (32) has been identified in the central part of the *chs\_H1* promoter at positions -(331–337), and, in addition, its motifs can be recognized within H-boxes and *Myb*-like boxes, position 468–479 nucleotides upstream of the coding region (Figure 2B). Because the presence of these boxes could indicate efficient *Myb* regulation of the *chs\_H1* gene, we concentrated on the analysis of possible interaction of the *chs\_H1* gene with an activator of anthocyanin biosynthesis, namely, the *Myb* transcription factor, PAP1, from *A. thaliana*, valuable for phenylpropanoid biotechnology.

For functional analyses of the *chs\_H1* sequence, a series of plant expression vectors were constructed (Figure 3) and transformed into *A. tumefaciens*. For transient expression assays, we used the technique of plant leaf infiltration with mixtures of *A. tumefaciens* strains. To assay the *chs\_H1* promoter activity, the promoter part was reamplified and fused via *Nco*I and *Bam*H1 with tandemly arranged *gfp* and *gus* genes in the vector pBGF-0. The resulting vector pBGF-PH1 (Figure 3a) was then used for infiltration of *N. benthamiana* leaves. Four days post-

infiltration, the GUS activity in leaf homogenates was measured using a fluorimetric method. It was found that the GUS activity increased 24.8-fold in leaves coinfiltrated with the PAP1 construct (vector pLV-65, Figure 3c) compared to infiltration without PAP1, reaching  $12373 \pm 36$  pmol of MU per minute and per milligram of fresh mass. These results clearly indicate the functionality of the cloned *chs\_H1* promoter sequence and its inducibility in the presence of PAP1.

Additional constructs were prepared to assay the functionality of the whole *chs\_H1* gene. Construct pLV-66 (Figure 3d) contains the native *chs\_H1* gene with a 0.5-kb upstream promoter and a natural intron (clone No. 1539). This construct was compared to the 35S-driven *chs\_H1* CDS of clone No. 132 (vector pLV-64; Figure 3c), as well as to the promoterless sequence of clone No. 1539 (vector pLV-78; Figure 3f) and the native *chs\_H1* gene arranged as a tandem with the 35S-driven *pap1* (vector pLV-67; Figure 3e). After leaf infiltration, the levels of *chs\_H1* mRNA were measured using SQ RT-PCR with Exon2-specific primers designated as a1 and a2 (see the Materials and Methods section). No *N. benthamiana* chalcone synthase was detected and, furthermore, PCR products were also absent after infiltration with the promoterless *chs\_H1* construct or with the *pap1* construct. Application of the “native” *chs\_H1* led to accumulation of a specific PCR product hybridizing to the H1 probe, as seen from a typical experiment in Figure 4,

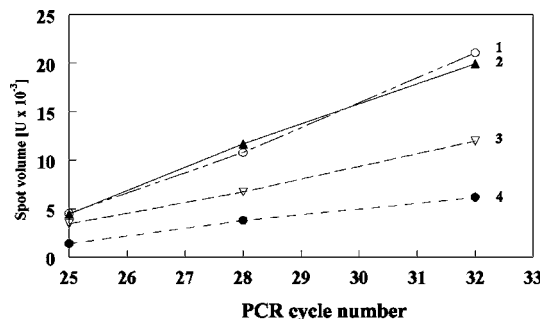


**Figure 4.** SQ RT-PCR analysis of the *chs\_H1* expression in infiltrated leaves of *N. benthamiana*. RNA was isolated from infiltrated leaf tissues of *N. benthamiana* 5 days post-infiltration, and aliquots of 1  $\mu$ g of RNA were analyzed by SQ RT-PCR reactions with the primers CHS\_H1 A1 and CHS\_H1 A2 (see the Materials and Methods section). Amplified products corresponding to cycle Nos. 25, 28, and 32 were analyzed by a Southern blot and quantified using a TYPHOON Phospholmager. The radioactivity signal is given in "volume" units that characterize pixel intensities (U) within the zone. (1) Sample from leaves infiltrated with the tandem construct of "native" *chs\_H1* and 35S-driven *pap1* (vector pLV-67). (2) Infiltration with 35S-driven *chs\_H1* (vector pLV-64). (3) Infiltration with a mixture of *Agrobacterium* strains bearing vectors pLV-66 ("native" *chs\_H1*) and pLV-65 (35S-driven *pap1*). (4) Infiltration with only "native" *chs\_H1* (vector pLV-66). No products and radioactivity signals were detected after infiltrations with only promoterless *chs\_H1* (vector pLV-78) or only 35S-driven *pap1* (vector pLV-67) or in control samples from noninfiltrated plants.

line 4, and this accumulation showed a higher rate when coinfiltration with the *pap1* gene was performed (Figure 4, line 3). Interestingly, the rate of *chs\_H1* mRNA accumulation was very high in samples infiltrated with *chs\_H1* and *pap1* arranged in tandem and reached almost the same rate as *chs\_H1* driven by the strong 35S promoter (compare lines 1 and 2, Figure 4). These results suggest, on the one hand, that some level of chalcone synthase transcription from the *chs\_H1* construct infiltrated into *N. benthamiana* leaves exists and, on the other hand, that this transcription is significantly enhanced by coapplication of the transcription factor PAP1.

A heterologous system of *P. hybrida* cv. Andrea producing blue-colored flowers was applied to monitor anthocyanin accumulation. To investigate the influence of PAP1 on petunia coloration, transgenic petunia lines were produced using the *A. tumefaciens* LBA 4404 bearing vector pLV-51 containing the *pap1* gene driven by the 35S promoter (for vector preparation, see the Materials and Methods section). Southern and Northern blots of selected petunia transgenotes that vigorously grew, rooted in media containing kanamycin, and expressed the *pap1* transgene are shown in Figure 5. These transgenotes exhibited a stable expression of *pap1* mRNA, while no hybridization signal was observed in tissues from nontransformed plants. A typical profile of the *pap1* mRNA expression is displayed in Figure 5B. The highest concentration of *pap1* mRNA was found in leaves, whereas very low concentrations appeared in mature flowers, suggesting a low transcription rate and/or a high mRNA turnover in flower corolla cells. The *pap1* transgenotes showed unusual coloration. Despite the high levels of *pap1* mRNA in young leaves, pigmentation was absent, while blue anthocyanin spots appeared in intermediate leaves and especially in the lower surface of old leaves (Figure 6, panels A and B). Blue pigmentation, which was absent in control plants, accumulated also on stem nodes, developing corolla and anthers, and in roots of in vitro transgenic plants. Analysis by light microscopy (Figure 6, panel G) showed that anthocyanins appeared both

in soluble forms and in specific inclusions in various parenchymatic tissues and in medulla, in which pigmentation was not observed in nontransformed controls (not shown). It is important to note that the intensity of coloration correlated with the intensity of sunlight and, as we found later, responded to UV-A irradiation (not shown).

In further experiments, infiltrations of young leaves of petunia controls and transgenotes with the *chs\_H1* and *pap1* constructs were combined with UV-A irradiation to detect the influence of these genes on anthocyanin production in petunia. The leaves were photographed after infiltration, and the intensity of the blue pigment was measured from electronic images by the color density option of the image analyzing program *Lucia* (see the Materials and Methods section). An increment of pixel mean density calculated from infiltrated versus control leaf tissues was plotted against the cultivation time post-infiltration, as shown in Figure 7, panel A. It should be noted that blue pigmentation appeared 5–6 days post-infiltration of control plants. In the absence of UV-A irradiation, the color was detectable only if the *chs\_H1* and *pap1* tandem was infiltrated (Figure 7, panel A, graph I). UV-A irradiation as a supplementary factor led to high pigment accumulation for the *chsH1* and *pap1* tandem variant and to moderate pigmentation after *chs\_H1* and *pap1* coinfiltration, while individual infiltration of *pap1*, 35S-driven *chs\_H1*, or "native" *chs\_H1* led to negligible coloration changes (Figure 7, panel A; compare graphs I and II). Interestingly, the blue coloration reached a maximum 6 days post-infiltration and then disappeared slowly, suggesting anthocyanin degradation or changes in young infiltrated petunia leaves (Figure 7, panel A). A quick leaf coloration response was achieved after infiltration of the *chs\_H1* and *pap1* tandem construct in young leaves of petunia transgenic lines. In this case, an intensive coloration appeared 2 days post-infiltration followed by a period of 12 h of post-UV-A irradiation (Figure 7, panel B), and then it disappeared slowly. These results indicate activation of the *chs\_H1* gene by the PAP1 coexpression, as well as a direct involvement of *chs\_H1* in transient pigment production in petunia. Moreover, *chs\_H1*-mediated pigmentation in petunia was stimulated by UV-A irradiation.

**Activation of *chs\_H1* due to UV-A Irradiation and Accumulation of Secondary Metabolites in hop Leaves.** Having experimental data on the stimulatory effect of UV-A irradiation on *chs\_H1*-mediated petunia leaf coloration, we addressed the issue of the possible activation of *chs\_H1* by UV-A irradiation of hop leaves. We reported previously that the level of *chs\_H1* is negligible in young hop leaves, especially in plants grown in greenhouse conditions under a low intensity of natural light (11). This low *chs\_H1* background enabled us to follow up on the effects of UV-A irradiation. Hop leaves were irradiated two times prior to collection, each time for 15 min in the middle of a regular 16-h photoperiod, followed by 1 day of additional cultivation. SQ RT-PCR gave higher rates of PCR product accumulation for RNA samples from UV-A-irradiated tissue in comparison to control samples exposed only to the standard illumination. This increase was in the range of 190–350% in comparison to controls (100%) depending on the experiment. To assay possible changes in the contents of secondary metabolites in irradiated leaves, qualitative and quantitative analyses were performed by HPLC. While leaves contain only very low levels of prenylated flavonoids, the analysis was focused on flavonol glycosides (derived from kaempferol and quercetin) and phenolic acids. Substantial differences in UV-A-irradiated hop leaves were noted in comparison to the controls, in particular for flavonol glycosides

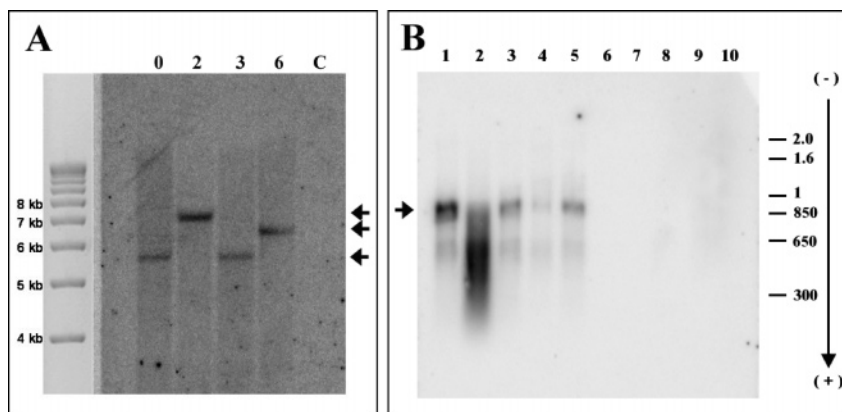


**Figure 5.** Southern blot (A) and Northern blot (B) analyses of *P. hybrida* transformed with *pap1*. (A) Genomic DNA was isolated from plant lines vigorously rooting in media-containing kanamycin ( $100 \text{ mg L}^{-1}$ ), digested with *Kpn*I, subjected to electrophoresis, blotted, and probed with a radioactivity-labeled *pap1* probe. Samples isolated from individual transgenic line Nos. 0, 2, 3, and 6 are designated by numbers on the top of the gel. “C” designates a sample from a nontransformed plant. The positions of hybridization signals confirming stable genomic integration of the transgene are indicated by arrows on the right side. The DNA marker (1-kb ladder, BRL) is positioned on the left side. (B) The total RNA was isolated from various tissues of the transgenic line No. 0 and subjected to Northern blot analysis (see the Material and Methods section): lane 1, RNA from young leaves; lane 2, old leaves; lane 3, stems; lane 4, fully expanded flower corollas; lane 5, roots. In lanes 6–10, tissue samples from nontransformed plants were applied. The smear in lane 2 is due to degradation of mRNA in old yellowish leaves from plants approximately 3 months after their transfer to the soil from in vitro culture and not due to the RNA extraction itself. The position of the full-length PAP1 mRNA signal is indicated by the arrow on the right side. The positions of the RNA molecular weight marker III (Boehringer, Mannheim, Germany) are shown on the right side.

with much higher amounts (8–25-fold) in the irradiated samples when compared to the controls (Table 1). The analysis of phenolic acids showed an opposite effect of UV-A irradiation. The normalized peak areas for phenolic acids are lower (0.3–0.6-fold) after UV-A exposure (Table 1). The only exception is a peak with a retention time of 13.4 min, which is 3-fold more concentrated in the irradiated samples.

## DISCUSSION

In this study, we aimed at characterizing oligofamily members of the hop genes encoding “true” chalcone synthase (EC 2.3.1.74). The main interest in this oligofamily, which was designated as *chs\_H1* according to the first sequence (AJ304877) isolated and analyzed previously (11, 12, 14), resides in its candidate role in the biosynthesis of bioactive prenylated flavonoids in hop (33). More specifically, prenylated chalcones have been characterized as highly valuable medicinal compounds (5, 6). On the basis of genomic blots, RFLP, and intron length polymorphism, it has been predicted that at least six distinct *chs\_H1*-hybridizing sequences would be present in hop cv. Osvald’s 72 (11, 12). However, it is uncertain whether or not some of these oligofamily members could be pseudogenes because at least two double-cleaved RFLP fragments hybridized only to an Exon1-specific probe (12). This observation could be attributed to full or partial deletion of Exon2. In the present study, we applied screening of a cDNA library derived from lupulin glandular tissue-enriched hop cone mRNA, which resulted in the isolation of two related clones No. 211 and No. 132 in addition to the original *chs\_H1* sequence. According to the screening, clone No. 132 seemed to be most abundant in the cDNA library, suggesting some quantitative differences in the expression of *chs\_H1* genes. In parallel, an additional complete *chs\_H1* gene variant (clone No. 1539) including promoter and intron sequences was amplified from hop genomic DNA. Sequential analysis of these four closely related *chs\_H1* sequence variants showed clearly that they are all matching a catalytic amino acid core that is characteristic for “true” chalcone synthases such as alfalfa CHS2, which has been analyzed by crystallography (34). The variability within three sequence

variants of the *chs\_H1* promoter was also very low, and all predicted cis elements were conserved in this 0.5-kb upstream promoter sequence. The major difference among promoter sequences appeared in the AT-rich region, in which deletions and base changes were found. Whether or not this AT-rich region or some more distant cis elements contribute to possible quantitative differences in the expression of this oligofamily in hop tissue is not known. The high uniformity of the characterized 0.5-kb upstream *chs\_H1* promoter and the coding regions indicates a rather high potential for functional uniformity within this *chs\_H1* oligofamily and argues against strict specialization of individual oligofamily members either in anthocyanin pigmentation in specific cells or in the accumulation of prenylated chalcones including X and DMX in hop lupulin glands. This assumption is consistent with the coexpression of *chs\_H1* sequences, which was observed also in our earlier studies using temperature-gradient gel analysis (11).

Despite the high uniformity of the *chs\_H1* oligofamily, there are considerable quantitative tissue-specific and developmental differences in *chs\_H1* mRNA levels in hop, and the level of this mRNA in lupulin glands is about 100-fold more concentrated than that in young leaves (11, 12). In addition, there are clear differences among different hop genotypes in their ability to produce prenylated chalcones (3, 12, 13), which, however, do not correlate with the number of predicted *chs\_H1* genes. It follows that various regulatory factors may be involved in the *chs\_H1* expression. Indeed, analysis of the *chs\_H1* promoter revealed several cis-regulatory elements characteristic for *chs* regulation (11) including *Myb*-binding sequences (13).

Rather than direct laborious and time-consuming hop transformation with *A. tumefaciens* (35), we used a very efficient transient expression assay in heterologous systems of *N. benthamiana* and *P. hybrida* via attached leaf infiltration (24). The aim was to study the responsiveness of the *chs\_H1* promoter and the whole gene to the coexpression of one of the conserved activators in the phenylpropanoid biosynthetic pathway, namely, the PAP1 factor from *A. thaliana* (15). Despite the prediction of the involvement of *myb* binding sites in the *chs\_H1* promoter, activation with PAP1 could not be predicted *a priori* because

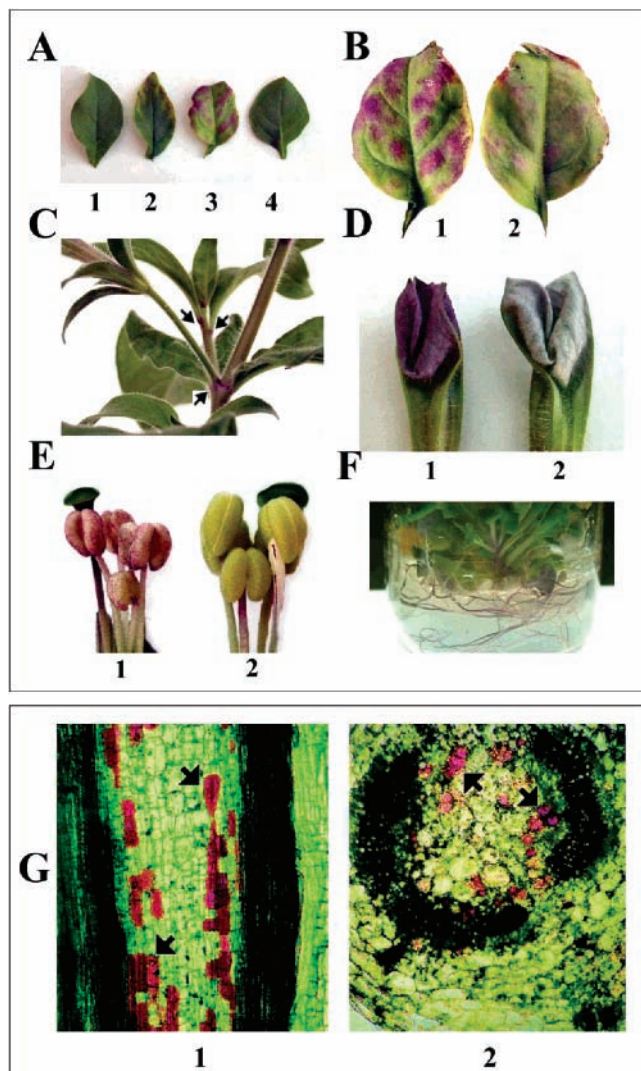


**Figure 6.** Analysis of anthocyanin coloration of transgenic petunia expressing the *pap1* gene. **A:** 1–3, young, intermediate, and old transgenic leaves, respectively; 4, old leaf from a nontransformed plant. **B:** details of pigmentation in an old leaf from the lower (1) and the upper (2) side. **C:** pigment accumulation in young stems; arrows show intense pigmentation in nodes and leaf abutement. **D:** more intense pigmentation in a developing transgenic corolla (1) than in a flower corolla of a nontransformed control (2). **E:** 1, pigmentation in transgenic anthers; 2, anthers of a nontransformed plant. **F:** blue roots of a transformed plant grown in vitro. **G:** longitudinal (1) and transverse (2) sections of stems of *pap1*-transformed petunia. Excised stems were sectioned and observed by light microscopy without staining. Pigment accumulation in medulla cells is shown by the arrows. Magnification: 51 $\times$ .

examples are known of the differential response of various chalcone synthase paralogues to the same *myb* activator in heterologous systems (4). In our experiments, coinfiltration of *pap1* driven by the 35S promoter with a chimeric construct containing the *chs\_H1* promoter fused to *gus* led unambiguously to an elevated GUS expression. In addition, coinfiltration with *pap1* led to the accumulation of *chs\_H1* mRNA in *N. benthamiana* leaves, suggesting PAP1-mediated activation of "natural" *chs\_H1*. This coinfiltration in petunia leaves led to the accumulation of blue-colored anthocyanins. This leaf coloration was inducible by UV-A that is a major UV component of the sunlight and occurred very fast in petunia transgenotes. Moreover, petunia transgenotes themselves showed unusual sunlight-

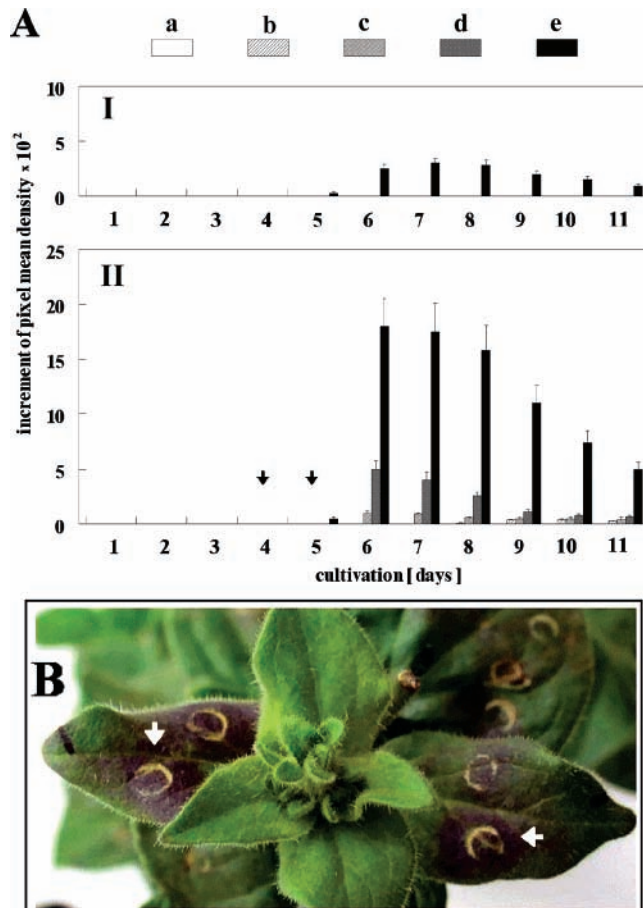


**Figure 7.** (A) Image analysis of pigmentation in infiltrated young petunia leaves. After infiltration, the leaves were photographed and the intensity of the blue color was measured from electronic images by the program *Lucia* (see the Materials and Methods section). An increment of a pixel mean density was calculated as the difference between coloration of infiltrated and control leaf tissues, and it was plotted against the cultivation time post-infiltration (panel A). At 4 and 5 days post-infiltration, UV-A irradiation of the leaves with a Black-Ray B100AP long-wave ultraviolet UV lamp was performed during 15 min as indicated by the arrows on graph II, while no UV-A irradiation was applied for graph I. Infiltrations were performed using the following vectors or vector combinations that correspond to the following column patterns: **a**, infiltration with the activation buffer (control sample); **b**, "native" *chs\_H1* gene (vector pLV-66); **c**, 35S-driven *pap1* gene (vector pLV-65); **d**, a mixture of "native" *chs\_H1* and 35S-driven *pap1* (see legend to Figure 4); **e**, "native" *chs\_H1* gene arranged in tandem with the 35S-driven *pap1* gene (vector pLV-67). (B) Leaf coloration of the transgenic petunia line 0 2 days post-infiltration with the vector pLV-67, followed by a period of 12-h post-UV-A irradiation. The infiltration zones are indicated by white arrows. The confidence intervals are given at  $\alpha = 0.05$ .

and UV-A-inducible patterns of pigment accumulation in various tissues and organs. All of these results suggest the involvement of additional petunia-specific and light-inducible regulatory factors that cointeracted in a combinatorial manner (36, 37) with 35S-driven *pap1* in the pathway to pigmentation. Some cointeracting factors could be Myc bHLH cofactors like JAF13 in petunia plants (19) or bZIP proteins that recognize specific G-boxes (38). At least two G-boxes were identified within the promoters of the *chs\_H1* oligofamily and, therefore, similar cofactors can interact directly with *chs\_H1*. The fact that UV-A light increased the accumulation of *chs\_H1* in hop leaves is consistent with a direct accumulation of flavonol glycosides in

**Table 1.** Normalized Peak Areas for Secondary Metabolites from hop cv. Osvald's 72 Clones

<i>t</i> <sub>R</sub> , min	Osvald's 72 irradiated <sup>a</sup>	Osvald's 72 control <sup>a</sup>	ratio irradiated vs control
Major Peaks at 350 nm ( <i>t</i> <sub>R</sub> = 10–30 min) (Flavonol Glycosides)			
17.8	29 785	3412	8.7
19.7	23 653	2260	10.5
21.8	70 879	6657	10.6
24.9	27 026	1068	25.3
Major Peaks at 310 nm ( <i>t</i> <sub>R</sub> = 10–20 min) (Phenolic Acids)			
11.4	31 836	51627	0.6
13.4	16 796	5468	3.1
16.1	6 934	21534	0.3
18.3	6 934	14247	0.5

<sup>a</sup> See the experimental procedures.

hop leaves found in our experiments. Furthermore, the lower levels of phenolic acids are also in accordance with an increase of the chalcone synthase activity due to consumption of their precursor, *p*-coumaroyl-CoA. The UV-A response of hop as well as of petunia is most probably regulated within the phototransduction pathways by a cryptochromes system homologous or analogous to CRY1 in *A. thaliana* (39, 40). We found very efficient *chs*\_H1 accumulation and blue pigmentation when the infiltration with *chs*\_H1 fused to *pap1* was performed in comparison to the response mediated by coinfiltration of these two genes as separate expression constructs. This difference can be explained by the fact that the fused construct is delivered by *A. tumefaciens* transformation in the same cells, while coinfiltration as a mixture can cause some degree of cellular and spatial separation of *chs*\_H1 and *pap1* expression constructs and, hence, a lower probability of interaction. An interesting finding is the temporal character of the induced leaf coloration, i.e., disappearance or degradation of anthocyanins or some other changes leading to loss of coloration. A similar effect was found, for instance, in leaf coloration of black-purple basil (*Ocimum basilicum* L.) after leaf shading (41). It is of interest to note that some transcription regulation factors like AN1 from petunia regulate not only the anthocyanin pathway in petunia anthers but also the anthocyanin acidification, which has an influence on the color of anthocyanins after deposition in vacuoles (42). The fast response was achieved after infiltration and irradiation of young leaves of petunia transgenotes. No blue pigment was usually seen on these leaves despite the detection of *pap1* mRNA on Northern blots. On the basis of the complexity of the PAP1 activity in *A. thaliana* (20), one can assume that, although blue coloration was not evident, some other changes preinduced by *pap1* in the petunia transcriptome most likely have led to significant acceleration of pigmentation after leaf infiltration with “native” *chs*\_H1 and the 35S-driven *pap1* tandem in combination with UV-A irradiation.

Taken together, we have shown that application of the PAP1 transcription factor, which is an orthologue of the petunia AN2 and maize C1 MYB factors (15), led to an elevated expression of the hop *chs*\_H1 gene in two species of the families of Solanaceae, *N. benthamiana*, and *P. hybrida*. This finding, together with the fact that the above-mentioned MYB factors coactivate pigmentation if expressed in evolutionary divergent heterologous systems (4), indicates that PAP1 activation of *chs*\_H1 will function in hop and, therefore, can be used in MYB biotechnology to modify the hop metabolome. Moreover, on the basis of the knowledge of the composition of the valerenone synthase promoter described by Okada et al. (43), which is unrelated to the *chs*\_H1 promoter and it is not UV-inducible,

one can expect that the expression of these two hop *chs* homologues should occur differentially under PAP1 coregulation. Differential or selective MYB activation of hop *chs* homologues and other genes will be a useful tool to study the biosynthetic pathways of valuable secondary metabolites in lupulin glands.

## ACKNOWLEDGMENT

We thank Helena Matoušková (BC IPMB, České Budějovice) for transformation of petunia plants and for excellent technical assistance. The authors are grateful to Dr. Petr Novák (BC IPMB, České Budějovice) for preparation of the pBFG-PH1 vector. The work was supported by Grants GAČR 521/03/0072, GAČR 521/06/P323, and AV0Z50510513, as well as by Grants MŠMT 1-2006-01 and 01S00906 (Special Research Fund of the Ghent University) within a bilateral collaboration research project between the Czech Republic and Flanders. Ina Janssens is thanked for assistance with sample preparations for HPLC analyses.

## LITERATURE CITED

- (1) Fukusaki, E.; Kobayashi, A. Plant metabolomics: potential for practical operation. *J. Biosci. Bioeng.* **2005**, *100*, 347–354.
- (2) Goodacre, R.; Vaidyanathan, V.; Dunn, W. B.; Harrigan, G. G.; Kell, D. B. Metabolomics by numbers: acquiring and understanding global metabolite data. *Trends Biotechnol.* **2004**, *22*, 245–252.
- (3) De Keukeleire, J.; Ooms, G.; Heyerick, A.; Roldán-Ruiz, I.; Van Bockstaele, E.; De Keukeleire, D. Formation and accumulation of  $\alpha$ -acids,  $\beta$ -acids, desmethylxanthohumol and xanthohumol during flowering of hops (*Humulus Lupulus* L.). *J. Agric. Food Chem.* **2003**, *51*, 4436–4441.
- (4) Broun, P. Transcription factors as tools for metabolic engineering in plants. *Curr. Opin. Plant Biol.* **2004**, *7*, 202–209.
- (5) Gerhäuser, C. Beer constituents as potential cancer chemopreventive agents. *Eur. J. Cancer* **2005**, *41*, 1941–1954.
- (6) Stevens, J. F.; Page, J. E. Xanthohumol and related prenylflavonoids from hops and beer: to your good health! *Phytochemistry* **2004**, *65*, 1317–1330.
- (7) Gerhäuser, C.; Alt, A.; Heiss, E.; Gamal-Eldeen, A.; Klimo, K.; Knauf, J.; Neumann, I.; Scherf, H. R.; Frank, N.; Bartsch, H.; Becker, H. Cancer chemopreventive activity of xanthohumol, a natural product derived from hop. *Molec. Cancer Ther.* **2002**, *1*, 959–969.
- (8) Miranda, C. L.; Stevens, J. F.; Helmrich, A.; Henderson, M. C.; Rodriguez, R. J.; Yang, Y. H.; Deinzer, M. L.; Barnes, D. W.; Buhler, D. R. Antiproliferative and cytotoxic effects of prenylated flavonoids from hops (*Humulus lupulus*) in human cancer cell lines. *Food Chem. Toxicol.* **1999**, *37*, 271–285.
- (9) Milligan, S. R.; Kalita, J. C.; Heyerick, A.; Rong, H.; De Cooman, L.; De Keukeleire, D. Identification of a potent phytoestrogen in hops (*Humulus lupulus* L.) and beer. *J. Clin. Endocrinol. Metab.* **1999**, *84*, 2249–2252.
- (10) Zuurbier, K. W. M.; Fung, S. Y.; Scheffer, J. J. C.; Verpoorte, R. *In vitro* prenylation of aromatic intermediates in the biosynthesis of bitter acids in *Humulus lupulus*. *Phytochemistry* **1998**, *49*, 2315–2322.
- (11) Matoušek, J.; Novák, P.; Patzak, J.; Bříza, J.; Krofta, K. Analysis of “true” chalcone synthase from *Humulus lupulus* L. and biotechnology aspects of “medicinal hops”. *Rostl. Výroba* **2002**, *48*, 7–14.
- (12) Matoušek, J.; Novák, P.; Bříza, J.; Patzak, J.; Niedermeierová, H. Cloning and characterization of *chs*-specific DNA and cDNA sequences from hop (*Humulus lupulus* L.). *Plant Sci.* **2002**, *162*, 1007–1018.

(13) Matoušek, J.; Vrba, L.; Novák, P.; Patzak, J.; De Keukeleire, J.; Škopek, J.; Heyerick, A.; Roldán-Ruiz, I.; De Keukeleire, D. Cloning and molecular analysis of the regulatory factor *HIMyb1* in hop (*Humulus lupulus L.*) and the potential of hop to produce bioactive prenylated flavonoids. *J. Agric. Food Chem.* **2005**, *53*, 4793–4798.

(14) Novák, P.; Krofta, K.; Matoušek, J. Chalcone synthase homologues from *Humulus lupulus*: some enzymatic properties and expression. *Biol. Plant.* **2006**, *50*, 48–54.

(15) Borevitz, J. O.; Xia, Y.; Blount, J.; Dixon, R. A.; Lamb, C. Activation tagging identifies a conserved MYB regulator of phenylpropanoid biosynthesis. *Plant Cell* **2000**, *12*, 2383–2394.

(16) Bovy, A.; de Vos, R.; Kemper, M.; Schijlen, E.; Pertejo, M. A.; Muir, S.; Collins, G.; Robinson, S.; Verhoeven, M.; Hughes, S.; Santos-Buelga, C.; van Tunen, A. High-flavonol tomatoes resulting from the heterologous expression of the maize transcription factor genes LC and C1. *Plant Cell* **2002**, *14*, 2509–2526.

(17) Lloyd, A. M.; Walbot, V.; Davis, R. W. *Arabidopsis* and *Nicotiana* anthocyanin production activated by maize regulators R and C1. *Science* **1992**, *258*, 1773–1775.

(18) Mathews, H.; Clendennen, S. K.; Caldwell, C. G.; Liu, X. L.; Connors, K.; Mattheis, N.; Schuster, D. K.; Menasco, D. J.; Wagoner, W.; Lightner, J.; Wagner, D. R. Activation tagging in tomato identifies a transcriptional regulator of anthocyanin biosynthesis, modification, and transport. *Plant Cell* **2003**, *15*, 1689–1703.

(19) Quattrocchio, F.; Wing, J. F.; van der Woude, K.; Mol, J. N.; Koes, R. Analysis of bHLH and MYB domain proteins: species-specific regulatory differences are caused by divergent evolution of target anthocyanin genes. *Plant J.* **1998**, *13*, 475–488.

(20) Tohge, T.; Nishiyama, Y.; Hirai, M. Y.; Yano, M.; Nakajima, J.; Awazuhara, M.; Inoue, E.; Takahashi, H.; Goodenow, D. B.; Kitayama, M.; Noji, M.; Yamazaki, M.; Saito, K. Functional genomics by integrated analysis of metabolome and transcriptome of *Arabidopsis* plants over-expressing an MYB transcription factor. *Plant J.* **2005**, *42*, 218–235.

(21) Töpfer, R.; Matzeit, V.; Gronenborn, B.; Schell, J.; Steinbiss, H. H. A set of plant expression vectors for transcriptional and translational fusions. *Nucleic Acids Res.* **1987**, *15*, 5890.

(22) Vrba, L.; Matoušek, J. Expression of modified 7SL RNA gene in transgenic *Solanum tuberosum* plants. *Biol. Plant.* **2005**, *49*, 371–380.

(23) Chytilová, E.; Macas, J.; Galbraith, D. W. Green fluorescent protein targeted to the nucleus, a transgenic phenotype useful for studies in plant biology. *Ann. Bot. (Oxford, U.K.)* **1999**, *83*, 645–654.

(24) Voinnet, O.; Rivas, S.; Mestre, P.; Baulcombe, D. An enhanced transient expression system in plants based on suppression of gene silencing by the p19 protein of tomato bushy stunt virus. *Plant J.* **2003**, *33*, 949–956.

(25) Murashige, T. F.; Skoog, F. A revised medium for rapid growth and bioassay with tobacco tissue cultures. *Physiol. Plant.* **1962**, *15*, 473–497.

(26) Horsch, R. B.; Fry, J. E.; Hoffman, N. L.; Eichholtz, D.; Rogers, S. G.; Fraley, R. T. A simple and general method for transferring genes into plants. *Science* **1985**, *227*, 1229–1231.

(27) Tai, T.; Tanksley, S. A rapid and inexpensive method for isolation of total DNA from dehydrated plant tissue. *Plant. Mol. Biol. Rep.* **1991**, *8*, 297–303.

(28) Church, G. M.; Gilbert, W. Genomic sequencing. *Proc. Natl. Acad. Sci. U.S.A.* **1984**, *81*, 1991–1995.

(29) Matoušek, J.; Trněná, L.; Svoboda, P.; Oriniaková, P.; Lichtenstein, C. P. The gradual reduction of viroid levels in hop mericlones following heat therapy: A possible role for a nuclease degrading dsRNA. *Biol. Chem. Hoppe-Seyler* **1995**, *376*, 715–721.

(30) Jefferson, R. A. Assaying chimeric genes in plants: the GUS gene fusion system. *Plant Mol. Biol. Rep.* **1987**, *5*, 387–405.

(31) Bork, P.; Brown, N. P.; Hegyi, H.; Schultz, J. The protein phosphatase 2C (PP2C) superfamily: detection of bacterial homologues. *Protein Sci.* **1996**, *5*, 1421–1425.

(32) Rushton, P. J.; Somssich, I. E. Transcriptional control of plant genes responsive to pathogens. *Curr. Opin. Plant Biol.* **1998**, *1*, 311–315.

(33) Etteldorf, N.; Becker, H. New chalcones from hop *Humulus lupulus* L. *Z. Naturforsch., C: J. Biosci.* **1999**, *54*, 610–612.

(34) Ferrer, J. L.; Jez, J. M.; Bowman, M. E.; Dixon, R. A.; Noel, J. P. Structure of chalcone synthase and the molecular basis of plant polyketide biosynthesis. *Nat. Struct. Biol.* **1999**, *6*, 775–784.

(35) Horlemann, C.; Schweißendieck, A.; Höhnle, M.; Weber, G. Regeneration and *Agrobacterium*-mediated transformation of hop (*Humulus lupulus* L.). *Plant Cell Rep.* **2003**, *22*, 210–217.

(36) Singh, K. B. Transcriptional regulation in plants: the importance of combinatorial control. *Plant Physiol.* **1998**, *118*, 1111–1120.

(37) Yamazaki, M.; Makita, Y.; Springob, K.; Saito, K. Regulatory mechanisms for anthocyanin biosynthesis in chemotypes of *Perilla frutescens* var. *crispa*. *Biochem. Eng. J.* **2003**, *14*, 191–197.

(38) Feldbrügge, M.; Sprenger, M.; Dinkelbach, M.; Yazaki, K.; Harter, K.; Weisshaar, B. Functional analysis of a light-responsive plant bZIP transcriptional regulator. *Plant Cell* **1994**, *6*, 1607–1621.

(39) Fuglevand, G.; Jackson, J. A.; Jenkins, G. I. UV-B, UV-A, and blue light signal transduction pathways interact synergistically to regulate chalcone synthase gene expression in *Arabidopsis*. *Plant Cell* **1996**, *8*, 2347–2357.

(40) Wade, H. K.; Bibikova, T. N.; Valentine, W. J.; Jenkins, G. I. Interactions within a network of phytochrome, cryptochrome and UV-B phototransduction pathways regulate chalcone synthase gene expression in *Arabidopsis* leaf tissue. *Plant J.* **2001**, *25*, 675–685.

(41) Phippen, W. B.; Simon, J. E. Anthocyanin inheritance and instability in purple basil (*Ocimum basilicum* L.). *J. Hered.* **2000**, *91*, 289–296.

(42) Spelt, C.; Quattrocchio, F.; Mol, J.; Koes, R. ANTHOCYANIN1 of petunia controls pigment synthesis, vacuolar pH, and seed coat development by genetically distinct mechanisms. *Plant Cell* **2002**, *14*, 2121–2135.

(43) Okada, Y.; Saeki, K.; Inaba, A.; Suda, N.; Kaneko, T.; Ito, K. Construction of gene expression system in hop (*Humulus lupulus*) lupulin gland using valerenophenone synthase promoter. *J. Plant Physiol.* **2003**, *160*, 1101–1108.

Received for review June 26, 2006. Revised manuscript received July 27, 2006. Accepted July 31, 2006.

JF061785G